A Slot Antenna Array With Low Mutual Coupling for Use on Small Mobile Terminals

Sema Dumanli, *Member, IEEE*, Chris J. Railton, and Dominique L. Paul, *Member, IEEE*

***Abstract*—In order to take full advantage of the benefits to be obtained by using MIMO techniques for mobile communications, it is necessary to use an antenna array which is both compact and also has low mutual coupling between ports. Generally these requirements are conflicting and to achieve them simultaneously is the subject of much research. In this paper a novel design for a two element cavity backed slot (CBS) array is described which has a measured mutual coupling of less than -15 dB despite an element spacing of only $\lambda/6$. This is achieved by adding a simple and easily manufactured meandering trombone structure to an existing CBS array which carries a portion of the input signal to the feed of the neighboring element. Measured and simulated results are presented for the behavior of the antenna and predictions are presented for the achievable channel capacity in several realistic scenarios.**

***Index Terms*—MIMO, slot antenna array.**

I. Introduction

With the steadily growing demand for information to be delivered to mobile terminals and handsets, there is an increasing need to maximize the use of the available bandwidth. One way of achieving this is to use multiple antenna elements at each end of the communications link. In situations where there is plenty of space, such as at mobile phone base stations or on laptop computers, it is not difficult to accommodate an antenna array. On small terminals, however, such as PDAs and mobile phones, it can be a challenge to fit in even a single antenna element since the size of the unit may be of the order of a wavelength. Any array of elements placed in such an environment must, therefore, by necessity be very closely spaced and is likely, therefore, to have an undesirably high mutual coupling.

Various techniques have been proposed in order to mitigate this problem. A comprehensive list of references for these is given in [1]. These include choosing the optimum position of the antennas on the PCB board to minimize the mutual coupling between elements [2] or shaping the PCB in some way either by cutting slots or by adding protrusions [3], [4]. Another approach is to add an external decoupling network, such as a rat race hybrid as used in [5]. In this case one of the ports feeds the elements in phase while the other feeds the elements in anti-phase [6]–[10]. While this method has been shown to give good results for the desired low mutual coupling, it has the disadvantage that the ports are asymmetrical and also that there can be problems with low bandwidth for the anti-phase port.

A more recent and very promising approach is to add an extra structure to the array in order to intentionally couple a small amount of the energy from one element to another. This can be done in such a way as to cancel the mutual coupling. An example of the use of this general approach for PIFA type elements is given in [11] but the proposed structure is very complicated. Another example is given in [12] but this involves a thin suspended stripline which may cause problems in robustness. In this paper a simple and robust method of achieving mutual coupling cancellation in a pair of closely spaced cavity backed slot (CBS) antennas is described. It is shown that even for a spacing of only $\lambda/6$, a measured mutual coupling of less than -15 dB was obtained together with a reflection of less than -25 dB at the operating frequency of 5.2 GHz. This can be compared to a measured mutual coupling of -7 dB and reflection of -12 dB for the same array without cancellation. In addition, in contrast to the situation when the rat-race hybrid is used, the symmetry and the bandwidth of the antenna are preserved.

II. The Array Element

It has been shown that CBS antennas are good candidates for MIMO systems since they are as efficient as monopole antennas [13] and arrays of CBS antenna elements have low mutual coupling [14]. They offer good MIMO capacities compared to competing designs such as the planar inverted-F (PIFA), and the dielectric resonator antenna (DRA) because of their high efficiency [13], [15]. In addition, if the cavity walls of the antenna are formed by using a curtain of shorting pins instead of solid copper a more accurate and repeatable manufacturing process is obtained without adversely affecting the mutual coupling [16]. For this reason, it was decided to design an array of two of these elements for use on a small mobile terminal and to include a cancellation structure in order to provide a low mutual coupling without compromising the available bandwidth. It is readily possible to extend this to a four element array by using the configuration of [17].

The geometry of the CBS element is shown in Fig. 1 and a two element array formed by placing two elements side by side is illustrated in Fig. 2. This was the structure developed in [16] which used the fewest shorting pins without degrading the mutual coupling as compared to using solid copper walls. Pins with

Manuscript received February 24, 2010; revised October 26, 2010; accepted October 26, 2010. Date of publication March 03, 2011; date of current version May 04, 2011. The work of S. Dumanli was supported by a postgraduate scholarship from Toshiba Research Europe Limited and The Scientific and Technological Research Council of Turkey (TUBITAK).

S. Dumanli was with the Centre for Communications Research, University of Bristol, Bristol BS8 1UB, U.K. She is now with Toshiba Research Europe, Bristol BS1 4ND, U.K. (e-mail: s.dumanli@bristol.ac.uk).

C. J. Railton and D. L. Paul are with the Centre for Communications Research, University of Bristol, Bristol BS8 1UB, U.K. (e-mail: chris.railton@bristol.ac.uk; d.l.paul@bristol.ac.uk).

Color versions of one or more of the figures in this paper are available online at http://ieeexplore.ieee.org.

Digital Object Identifier 10.1109/TAP.2011.2123057

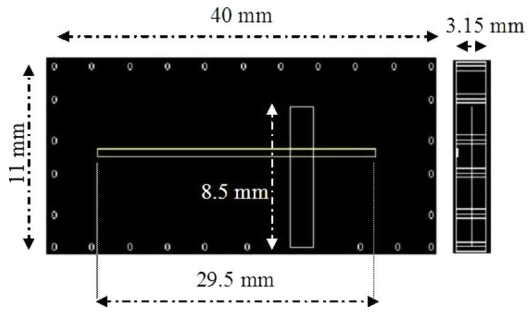

Fig. 1. The single CBS element to operate at 5.2 GHz.

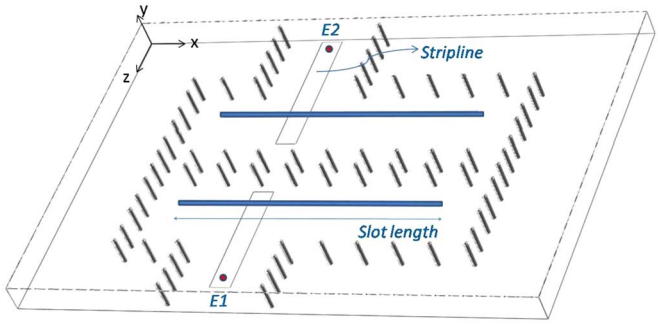

Fig. 2. A two element array of CBS elements.

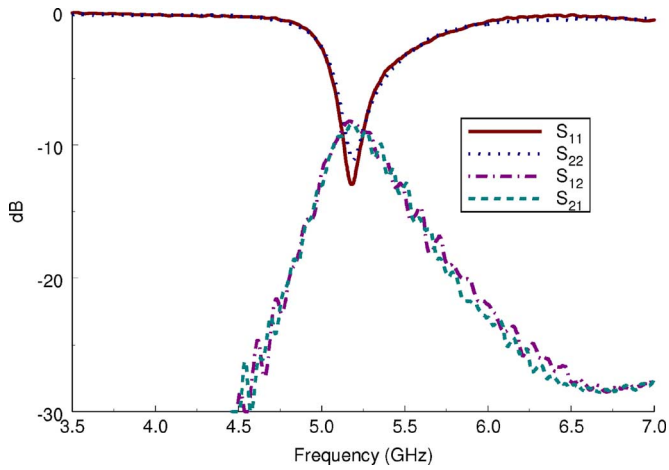

Fig. 3. Measured S parameters with no ground plane.

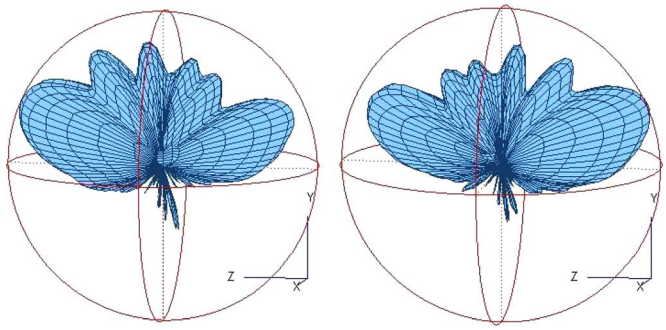

Fig. 4. Measured radiation patterns of the two embedded elements on a 15 cm ground plane.

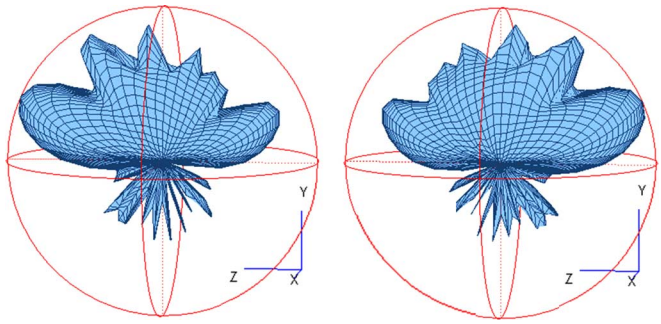

Fig. 5. Simulated radiation patterns of the two embedded elements on a 15 cm ground plane.

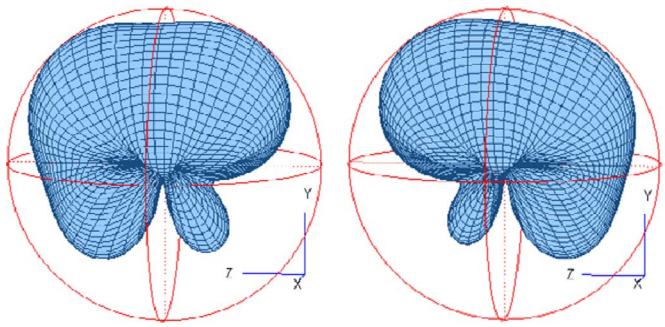

Fig. 6. Simulated radiation pattern patterns of the two embedded elements with no ground plane.

radius 0.275 mm with a separation of 4 mm were used. The measured S parameters of this array in Fig. 3 show a mutual coupling of −7 dB at 5.2 GHz. While this is still usable it does represent a power loss of approximately 25% so it is desirable for the coupling to be reduced. The measured and simulated radiation patterns of this array are shown in Figs. 4 and 5 which exhibit very good agreement with each other. To facilitate measurement, the array was placed on a ground plane of radius 15 cm. The effect of this is to make the radiation pattern more complicated due to diffraction effects but not to significantly alter the general features. The expected radiation pattern in the absence of a ground plane is shown in the simulated results of Fig. 6. In each case it can be seen that the effect of mutual coupling is to introduce a small amount of squint in the two patterns. This squinting of the radiation pattern is caused by the asymmetry of the structure. The slot which is not driven acts as a parasitic element which receives and re-radiates some of the energy thus distorting the radiation pattern. While it has been shown that the squint can be an advantage in MIMO and diversity systems [18], this is more than negated by the reduced radiation due to mutual coupling loss.

III. The Decoupling Structure

Several different possible structures were investigated and evaluated by means of extensive finite difference time domain (FDTD) simulations. This was done using the enhanced FDTD software developed at the University of Bristol which includes the facility to calculate S parameters and 3D far field radiation patterns of antennas. Of those tested, it was found that structure shown in Fig. 7 gave the best performance, the greatest ease of manufacture and the least sensitivity to manufacturing tolerances. In this scheme, the feed lines have been extended and

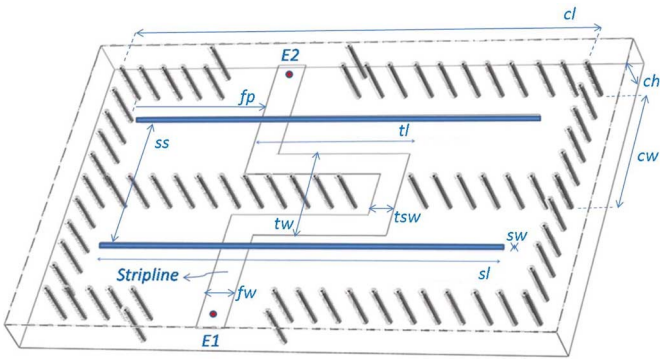

Fig. 7. Structure of the decoupled array.

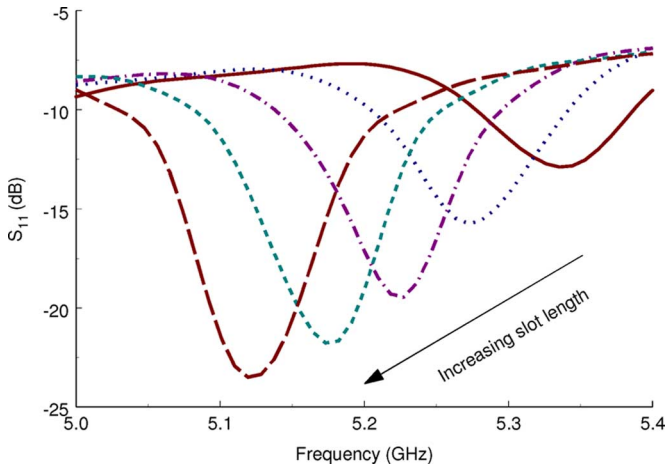

Fig. 8. S_{11} characteristics for slot lengths of 31 to 35 mm in 1 mm increments and trombone length of 11 mm.

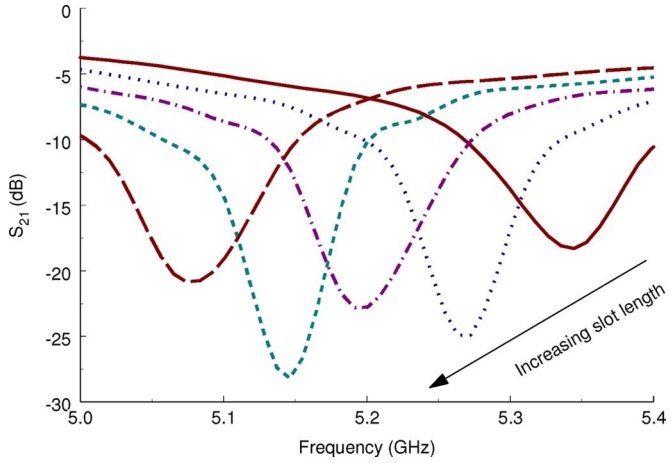

Fig. 9. S_{21} characteristics for slot lengths of 31 to 35 mm in 1 mm increments and trombone length of 11 mm.

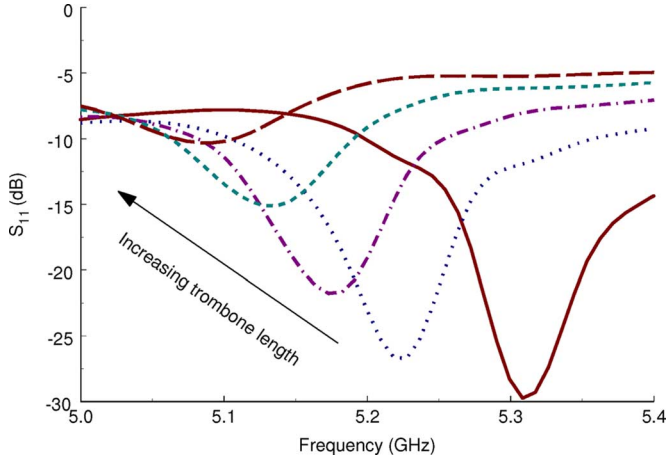

Fig. 10. S_{11} characteristics for trombone lengths of 10 mm to 12 mm in 0.5 mm increments and slot length of 35 mm.

joined with a meandering "trombone" section which carries a portion of the input signal from the excited feed to the neighboring element. With an appropriate choice of dimensions, it is shown that the signal coupled through the trombone can be made to cancel the original mutual coupling yielding a pair of well isolated ports. In order to find the optimum dimensions for the trombone section, a parametric study was done using FDTD simulations. There are a number of parameters which can be chosen in order to give the required magnitude and phase for the coupled signal. Primarily, these are the width and length of the strip making up the trombone section and the length of the slot.

Typical results for different slot lengths and trombone lengths are shown in Figs. 8–11. In Fig. 8 it is shown that the frequency at which the minimum reflection is obtained, is lower as the slot is lengthened. Also it can be seen that the match improves as the slot is lengthened. Fig. 9 shows that the frequency at which the mutual coupling is lowest also reduces monotonically as the slot is lengthened but that the level of the minimum is approximately constant. Also it can be seen that the dependence of the frequency on length is not the same for S_{11} as for S_{21}. Thus there exists a slot length at which the two minima are at the same frequency. If this frequency can be made equal to the desired operating frequency, this will be the best choice.

The effect of the trombone length is more complex as this affects both the matching of the element and also the magnitude and phase of the coupling between elements. Fig. 10 shows the dependence of S_{11} on trombone length. It can be seen that this length has a considerable effect both on the center frequency and also on the matching. Finally Fig. 11 shows the effect of trombone length on mutual coupling. In this case the effect on the frequency of the minimum is weaker but more complicated.

The effect of varying other parameters such as the width of the trombone line and the size of the cavity were also investigated but in most cases no particular advantage or disadvantage was to be gained by changing these. It was found that best results were achieved under the following conditions.

1. The width of the stripline making up the trombone was similar to the width of the feedline. This led to the antenna characteristic being not unduly sensitive to manufacturing tolerances. Narrower trombone widths could be used but the exact dimensions were more critical.
2. The side arms of the trombone section were centrally placed between the radiating slot and the central row of shorting pins. If they were not placed in this position, the coupling between the side arms and the slot or pins led to the results being sensitive to manufacturing tolerances.

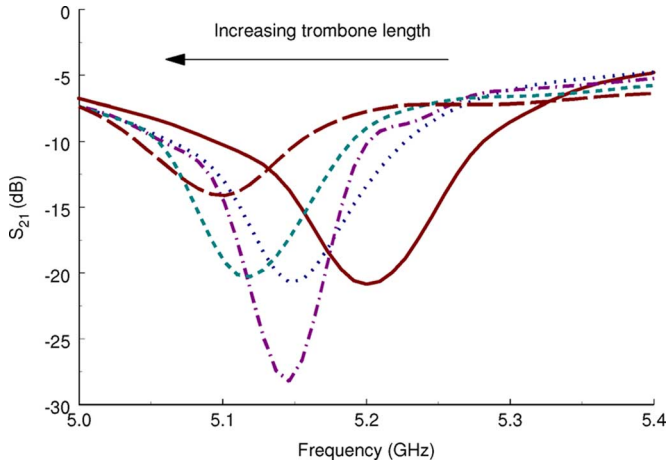

Fig. 11. S_{21} characteristics for trombone lengths of 10 mm to 12 mm in 0.5 mm increments and slot length of 35 mm.

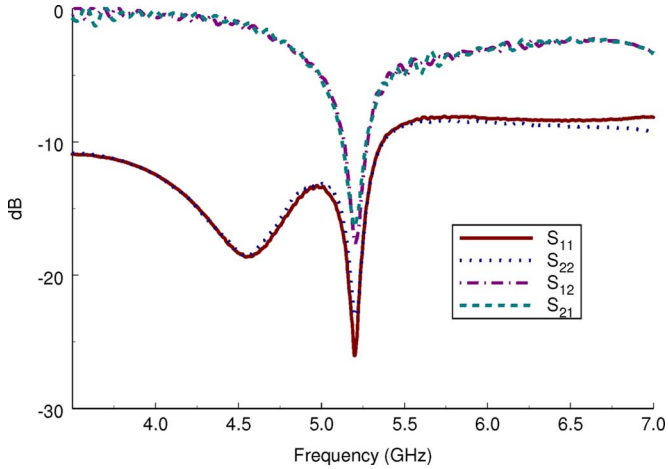

Fig. 13. Measured S parameters of the final array.

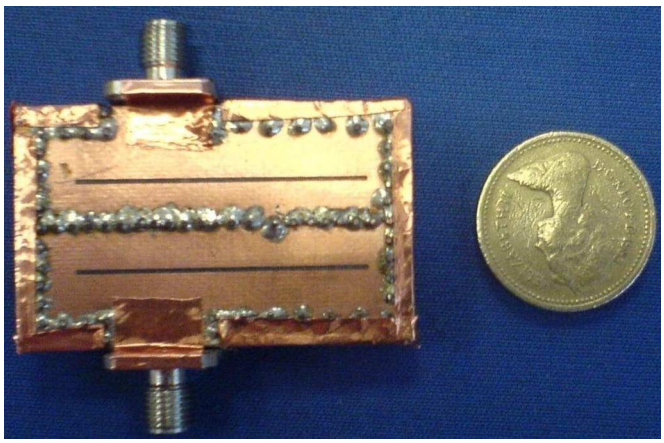

Fig. 12. The manufactured decoupled array.

TABLE I
DIMENSIONS OF THE FINAL DECOUPLED ARRAY IN MM

cavity length (cl)	40	slot separation (ss)	12
cavity width (cw)	11	trombone length (tl)	13.65
cavity height (ch)	3.15	trombone strip width (tsw)	2
slot width (sw)	0.5	trombone width (tw)	8
slot length (sl)	34	dielectric constant	2.2
feed width (fw)	2.6	feed position (fp)	12

Given these constraints, the dimensions for the final design were arrived at by means of the results of the FDTD parametric analysis.

IV. THE FINAL ARRAY

The final manufactured array is illustrated in Fig. 12 and has the dimensions given in Table I. The feed position is the distance between the bottom of the slot and the bottom of the feed line as shown in Fig. 7.

It is noted that the slot length of the final array is considerably longer than in the original un-decoupled array. This was necessary in order to obtain the correct center frequency. It is also noted that whereas the manufactured test antenna is fitted with SMA connectors, the connections would normally be directly made with the RF circuitry.

Measurements of the antenna S parameters and radiation patterns were made using the Department's anechoic chamber and an Anritsu 37397C Vector Network Analyser. In order to measure the 3D radiation patterns, a Flann DP-240AA horn antenna was used as a reference and a pair or orthogonally mounted stepper motors were used to scan the antenna under test in the azimuth and elevation directions. The resulting data was collected and plotted using in-house MATLAB codes. Full details of the equipment and the test setup can be found in [19] and [20].

The measured S parameters for the final manufactured array are shown in Fig. 13. It can be seen that the mutual coupling has been reduced to less than -15 dB and the reflection has been improved over that of the original single element and is now less than -20 dB. Measured and simulated radiation patterns using a model which includes the 15 cm ground plane are shown in Figs. 14 and 15 where good agreement can be seen. The simulated result for the case where there is no ground plane is shown in Fig. 16. In all cases it can be seen that the radiation pattern exhibits a strong squint despite the low mutual coupling. In this case the asymmetry is introduced because the element which is not driven directly is fed with a small amount of power through the trombone structure. The superposition of the main beam and the radiation from the second element results in an asymmetrical squinted radiation pattern. This behavior can be advantageous in providing pattern diversity or a low envelope correlation when used in MIMO systems.

Figs. 17 and 18 show the current distribution on the antenna feeds for the original array of Fig. 2 and for the final array of Fig. 7. It can be clearly seen that the current on the victim feed is much less for the final array than for the original. Moreover, the cancellation effect between the trombone current and the energy coupled through the victim slot is apparent as the current sharply reduces when the feed line crosses the position of the slot.

Where the array is to be used in a MIMO system, the envelope correlation coefficient is a relevant characteristic. This property was calculated for the original non-decoupled array and for the

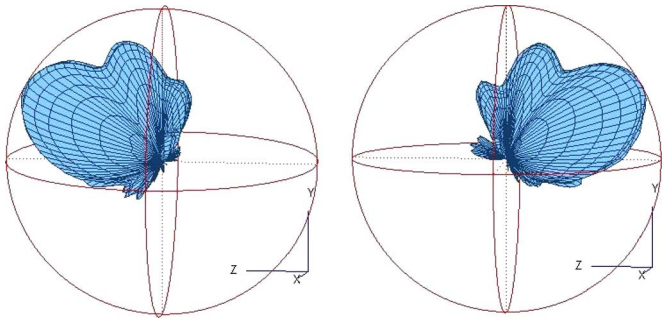

Fig. 14. Measured radiation patterns of the two embedded elements on a 15 cm ground plane.

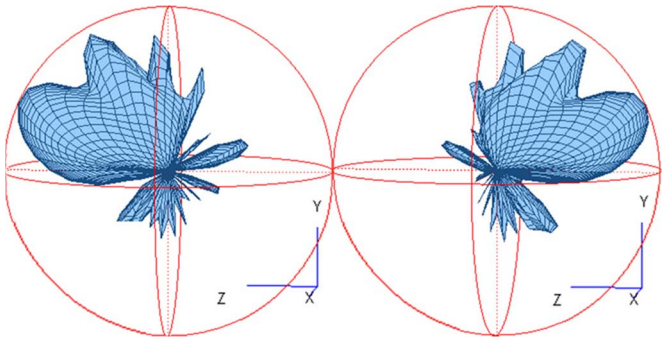

Fig. 15. Simulated radiation patterns of the two embedded elements on a 15 cm ground plane.

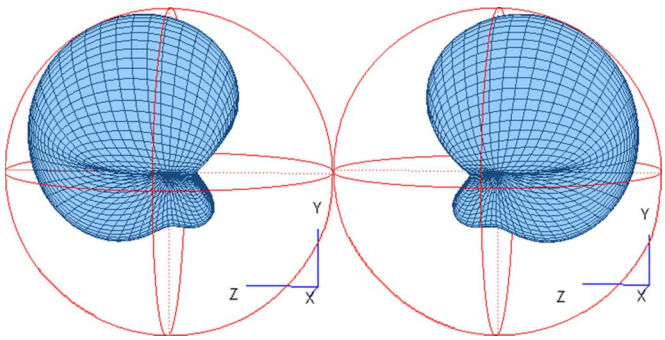

Fig. 16. Simulated radiation patterns of the two embedded elements with no ground plane.

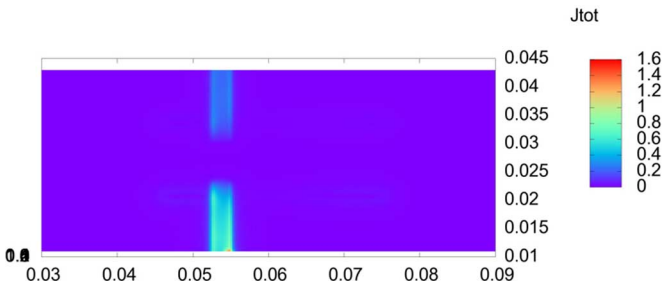

Fig. 17. Current distribution on feeds for original array.

final array using the measured S parameters and (1) and (2). The method is based on that described in [21].

$$\rho_{i,j} = \frac{|P_{i,j}|}{\sqrt{|P_{i,i}||P_{j,j}|}} \tag{1}$$

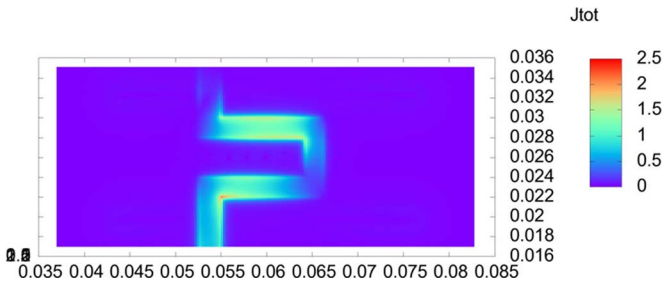

Fig. 18. Current distribution on feeds for trombone array.

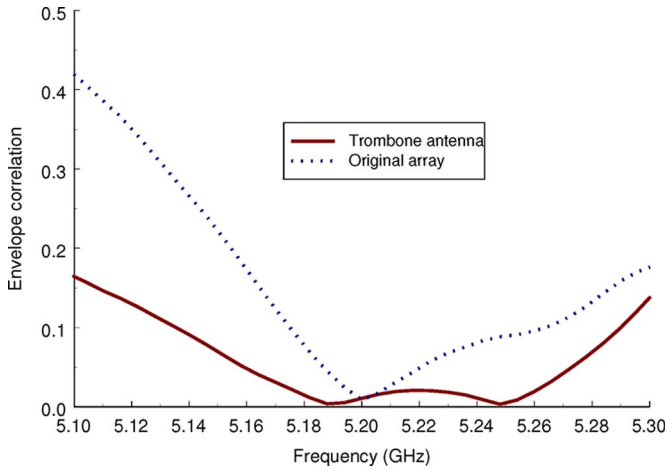

Fig. 19. Measured envelope correlation of the original and final arrays.

where

$$P = I - SS^H. \tag{2}$$

Although this method is strictly valid only for lossless antennas, in this case the measured efficiency was high so this method can still be used with good accuracy. In Fig. 19, it can be seen that the envelope correlation is improved over that of the original array and that it remains low over a wider frequency range.

V. Efficiency Measurements

The efficiency of the final trombone array and the original array were measured. This was done by comparing the radiated power from the test antenna with that obtained from an element which is known to have a high efficiency, in this case a monopole. In order to achieve as much accuracy as possible, the measurements were made on the same day in the same anechoic chamber and three sets of measurements were made. Finally the total radiated powers are averaged and compared. This method is expected to have less than a 5% uncertainty. In addition, the efficiency was calculated from the FDTD results using a perturbation method. The results are given in Tables II and III with mismatch loss excluded and included respectively. It can be seen that good agreement exists between measurement and calculation.

The calculated losses from the conductors and the dielectrics are given in Table IV.

It can be seen that the extra loss associated with the trombone is due to extra losses in the conductors. Nevertheless, this loss

TABLE II
MEASURED AND CALCULATED EFFICIENCIES EXCLUDING MISMATCH LOSS

	Trombone	Original array
Measured efficiency	82%	93%
Calculated efficiency	80%	88%

TABLE III
MEASURED AND CALCULATED EFFICIENCIES INCLUDING MISMATCH LOSS

	Trombone	Original array
Measured efficiency	80%	74%
Calculated efficiency	79%	74%

TABLE IV
CALCULATED DIELECTRIC AND CONDUCTOR LOSS

	Trombone	Original array
Conductor loss	19%	10%
Dielectric loss	1.3%	1.3%

Fig. 20. The channel model for comparing antenna performance.

is more than made up for by the reduction of mutual coupling loss.

VI. THE ARRAY AS PART OF A MIMO SYSTEM

In order to assess the performance of the antenna in a real situation compared with the original array, the system performance was simulated using a number of different measured and statistically generated channels.

The channel model which was used is shown in Fig. 20 which is a 2 N port network where N is the number of receive and transmit elements. This network can be described by an S matrix with the following structure

$$S^{\mathrm{tot}} = \begin{pmatrix} R_{\mathrm{tx}} & H \\ H^T & R_{\mathrm{rx}} \end{pmatrix} \tag{3}$$

where H is the channel matrix while $\mathrm{R_{tx}}$ and $\mathrm{R_{rx}}$ are the individual S matrices of the transmit and receive arrays respectively.

In each case, the channel was expressed as the summation of paths such that the total received signal was the superposition of a number of plane waves. The H matrix which characterizes the transmission from the terminals of the transmit antenna array to those of the receive antenna array is given by

$$H_{ij} = \sum_k A_k e^{j\psi_k} G_{\mathrm{tx}}(\theta d_j, \varphi d_j) G_{\mathrm{rx}}(\theta i_i, \varphi i_i) \tag{4}$$

where $\theta i, \phi i, \theta d, \phi d$ are the elevation and azimuth angles of arrival and departure respectively. $G(\theta, \phi)$ is the embedded gain of the element in the direction. $\mathrm{A_k}$ is the attenuation of the path. The statistical distributions of these parameters will depend upon the channel being used. For the results presented in this paper, the distributions are given below.

It is common practice to normalize the channel matrix to a "unit gain" channel as shown in (5)

$$\hat{H} \leftarrow \frac{H}{\sqrt{\sum_i \sum_j |H_{ij}|^2}} \tag{5}$$

where the summations are taken over all elements of the H matrix. This, however, includes the effects of the antenna so that issues such as return and mutual coupling loss are masked. In this work, following [22], the alternative normalization given by (6) is used

$$\hat{H} \leftarrow \frac{H}{\sqrt{\sum_k |A_k|^2}}. \tag{6}$$

Here, the summations are taken over all paths in the channel model. It is noted that this normalization does not involve the properties of the antenna, such as the radiation pattern, the efficiency and return loss so it allows a realistic comparison between antenna systems. As described in [22], this is equivalent to ensuring unit normalized channel gain when ideal isotropic radiators are used. It is also comparable to the "link capacity" described in [23] as contrasted with the "MIMO capacity" also described in the same paper. The results presented in this paper are all calculated using this normalization.

Three different sets of channel data were used for comparison.

1. Artificial channel
   Firstly, the data for the channel was generated using a specified statistical distribution. This was an idealized test scenario where there was a very rich multi-path environment and a uniform distribution of angles of arrival for the received signals. All angles were uniformly distributed. The path lengths were normally distributed with a mean of 2 km and standard deviation of 200 m. Path loss and phase were calculated for a line of sight path of the same total length. 40 independent paths were assumed to exist and 1000 simulations were used in order to obtain the statistical properties.
2. Measured outdoor channel data [24]
   Tests were also carried out using real channel data measured in Bristol city center. Only the receive parameters were available so the transmit parameters were estimated. In particular the angle of departure was assumed to be uniformly distributed around the azimuthal plane. The azimuthal angle of arrival was distributed over a wide range but exhibited a peak in the direction of the transmitter. Fig. 21 shows the number of paths which arrive at different angles. The elevation angles were mostly close to the horizontal. A maximum number of 40 independent paths were allowed for, based on the measured information, and 100 simulations were done in order to obtain the statistical properties. Ideally, a greater number of simulations would have been used but this was limited by the available data.
3. Ray tracing data for an office environment [24]
   An in-house ray-tracing tool was used to obtain channel data for an open plan office at Bristol. In general it was

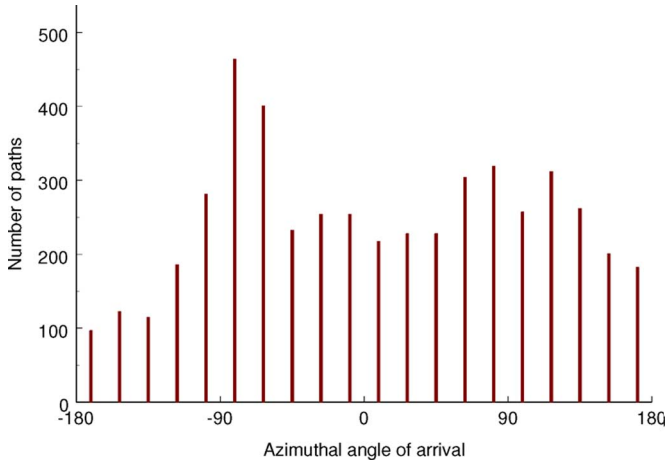

Fig. 21. Distribution of azimuth angles of arrival for outdoor channel.

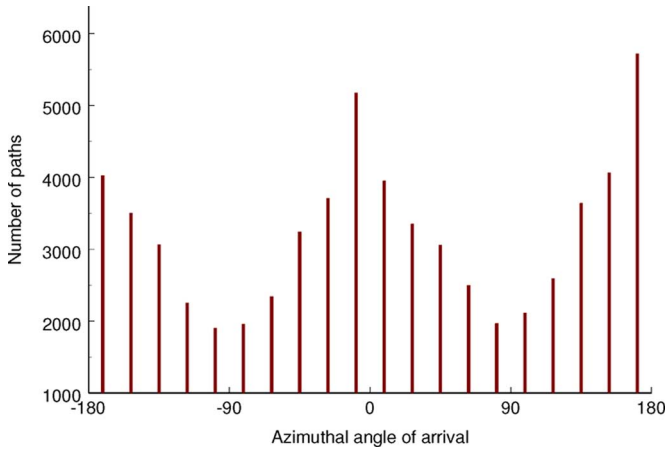

Fig. 22. Distribution of azimuth angles of arrival for indoor channel.

found that there were fewer then 6 significant independent paths. 10 000 simulations were used in order to obtain the statistical properties. For this case the angles of arrival showed strong peaks at angles determined by the furniture near the receiver as shown in Fig. 22.

The capacity was calculated using the following formula:

$$C = \log_2 \det\left(I + \sigma \hat{H}\overline{\hat{H}^T}\right). \tag{7}$$

The capacities were calculated with the signal to noise ratio, σ in (7), set to 20 dB. These are shown in Figs. 23–25 for the measured and the simulated channels and for the original array and the final array. Also, a comparison is given with an ideal independently identically distributed (IID) Rayleigh channel of the type studied in [25]. The results were calculated using in-house MathCad software which, for each simulation of the channel, applied (7) to ascertain the capacity. The CDFs in each case were then readily obtained. It can be seen that, in each case, there is a substantial improvement to be gained by using the cancellation network when the spacing between elements is small. It is noted that the results for the outdoor channel data are not as smooth as for the others. This is due to the low number of simulations which were available in this case.

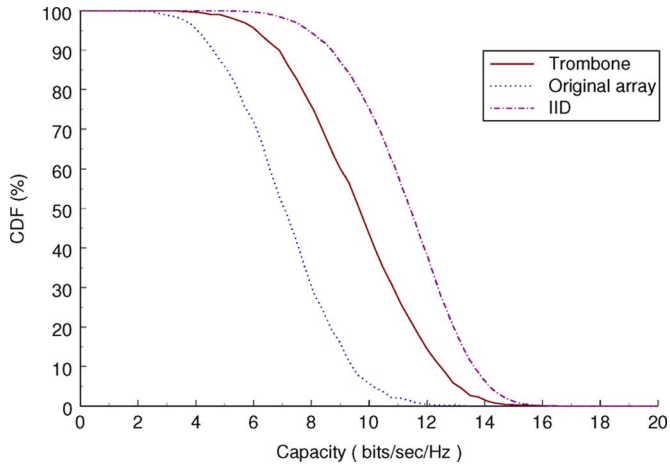

Fig. 23. Comparison of capacity for the two antennas for the artificial channel. The theoretical capacity for a 2×2 IID channel and isotropic antennas is given for comparison.

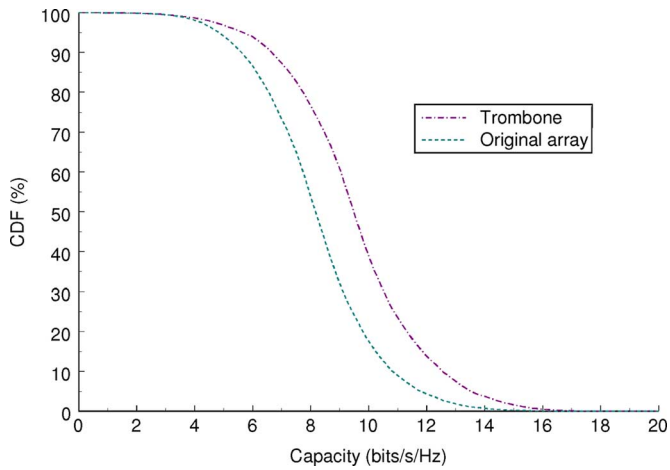

Fig. 24. Comparison of capacity for the two antennas for the ray-traced indoor channel.

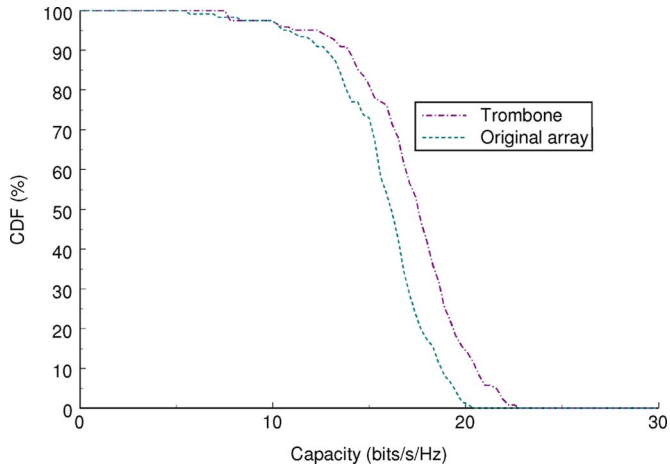

Fig. 25. Comparison of capacity for the two antennas for the measured outdoor channel.

VII. Conclusion

In this paper a novel slot antenna array with a mutual coupling of less than -15 dB and a reflection of less than -25 dB, despite

a separation of only $\lambda/6$, has been described. The decoupling has been achieved by adding a meandering trombone structure which is easy to manufacture and couples a small amount of energy from one element to the other so as to cancel the original mutual coupling. The result is a radiation pattern which is highly squinted and exhibits a low envelope correlation over a wide frequency range. This array, and other arrays of this type, are expected to have many applications for MIMO type systems on small terminals where there is not enough room for widely spaced array elements.

ACKNOWLEDGMENT

The authors would like to thank their colleagues in the Communications Systems and Networks Group, headed by Prof. J. McGeehan, for helpful discussions and for providing information on the measured and ray-traced channels.

REFERENCES

[1] C. Luxey, "Design of multi-antenna systems for UTMS mobile phones," in *Proc. Loughborough Antennas and Propagation Confe.*, Nov. 2009, pp. 57–64.

[2] S. Dumanli, Y. Tabak, C. Railton, D. Paul, and G. Hilton, "The effect of antenna position and environment on MIMO channel capacity for a 4 element array mounted on a PDA," in *Proc. 9th Eur. Conf. on Wireless Technology*, 2006, pp. 201–204.

[3] M. Karaboikis, C. Soras, G. Tsachtsiris, and V. Makios, "Compact dual-printed inverted-F antenna diversity systems for portable wireless devices," *IEEE Antennas Wireless Propag. Lett.*, vol. 3, pp. 9–14, 2004.

[4] T. Ohishi, N. Oodachi, S. Sekine, and H. Shoki, "A method to improve the correlation and the mutual coupling for diversity antenna," presented at the IEEE Antennas and Propagation Society Int. Symp., Washington, DC, Jul. 2005.

[5] S. Dumanli, C. Railton, and D. Paul, "A decorrelated closely spaced array of four slot antennas backed with SIW cavities for MIMO communications," in *Loughborough Antennas and Propagation Conf.*, Nov. 2009, pp. 277–280.

[6] S. Dossche, S. Blanch, and J. Romeu, "Decorrelation of a closely spaced four element antenna array," presented at the IEEE Antennas and Propagation Society Int. Symp., 2005.

[7] S. Dossche, S. Blanch, and J. Romeu, "Optimum antenna matching to minimise signal correlation on a two-port antenna diversity system," *IET Electron. Lett.*, vol. 40, no. 19, pp. 1164–1165, Sep. 2004.

[8] S. Dossche, J. Rodriguez, L. Jofre, S. Blanch, and J. Romeu, "Decoupling of a two-element switched dual band patch antenna for optimum MIMO capacity," in *Proc. Int. Symp. on Antennas and Propagations*, Albuquerque, NM, Jul. 2006, pp. 325–328.

[9] M. Shanawani, D. L. Paul, S. Dumanli, and C. Railton, "Design of a novel antenna array for MIMO applications," in *Proc. 3rd Int. Conf. on Information and Communication Technologies: From Theory to Applications ICTTA*, 2008, pp. 1–6.

[10] A. Nilsson, P. Bodlund, A. Stjernman, M. Johansson, and A. Derneryd, "Compensation network for optimizing antenna system for MIMO application," presented at the Eur. Conf. on Antennas and Propagations, Edinburgh, U.K., Nov. 2007.

[11] A. C. K. Mak, C. R. Rowell, and R. D. Murch, "Isolation enhancement between two closely packed antennas," *IEEE Trans. Antennas Propag.*, vol. 56, no. 11, pp. 3411–3419, Nov. 2008.

[12] A. Diallo, C. Luxey, P. Le Thuc, R. Staraj, and G. Kossiavas, "Study and reduction of the mutual coupling between two mobile phone PIF as operating in the DCS1800 and UMTS bands," *IEEE Trans. Antennas Propag.*, vol. 54, no. 11, pp. 3063–3074, Nov. 2006.

[13] G. S. Hilton and H. W. W. Hunt-Grubbe, "Simulation and practical analysis of a cavity-backed linear slot antenna for operation in the IEEE802.11a band," presented at the 5th Eur. Workshop on Conformal Antennas, Bristol, U.K., Sep. 2007.

[14] A. Hadidi and M. Hamid, "Aperture field and circuit parameters of cavity-backed slot radiator," in *IEE Proc. Microw., Antennas Propag.*, 1989, vol. 136, no. 2, pp. 139–146.

[15] A. Pal, C. Williams, G. Hilton, and M. Beach, "Evaluation of diversity antenna designs using ray tracing, measured radiation patterns, and MIMO channel measurements," *EURASIP J. Wireless Commun. Network.*, vol. 2007, no. 1, pp. 61–72, 2007.

[16] S. Dumanli, C. J. Railton, D. L. Paul, and G. S. Hilton, "Closely spaced array of cavity backed slot antennas with pin curtain walls," in *IET Proc.*, to be published.

[17] S. Dumanli, C. Railton, and D. Paul, "Decorrelation of a closely spaced antenna array and its influence on MIMO channel capacity," presented at the EuCAP, Edinburgh, U.K., Nov. 11–16, 2007.

[18] P. N. Fletcher, M. Dean, and A. R. Nix, "Mutual coupling in multi-element array antennas and its influence on MIMO channel capacity," *Electron. Lett.*, vol. 39, no. 4, pp. 342–344, Feb. 20, 2003.

[19] H. Hunt-Grubbe, "Element and integrated system analysis of a dual feed tuneable cavity backed linear slot antenna," Ph.D. dissertation, Univ. Bristol, Bristol, U.K., Mar. 2007.

[20] G. Hilton, "Basic use of VNAs and the anechoic chamber facility," Laboratory notes for Antennas and Electromagnetic Compatibility, Univ. Bristol, U.K.

[21] S. Blanch, J. Romeu, and I. Corbella, "Exact representation of antenna system diversity performance from input parameter description," *Electron. Lett.*, vol. 39, no. 9, pp. 705–707, May 1, 2003.

[22] A. Pal, C. Williams, G. Hilton, and M. Beach, "Evaluation of diversity antenna designs using ray tracing, measured radiation patterns and MIMO channel measurements," *EURASIP J. Wireless Commun. Network.*, vol. 2007, 58769, Article ID.

[23] V. Jungnickel, V. Pohl, and C. von Helmolt, "Capacity of MIMO systems with closely spaced antennas," *IEEE Commun. Lett.*, vol. 7, no. 8, pp. 361–363, Aug. 2003.

[24] M. Beach *et al.*, "An experimental evaluation of three candidate MIMO array designs for PDA devices," presented at the Joint COST 273/284 Workshop on Antennas and Related System Aspects I in Wireless Communications, Gothenburg, Sweden, Jun. 2004.

[25] G. J. Foschini and M. J. Gans, "On the limits of wireless communications in fading environment when using multiple antennas," *Wireless Pers. Commun.*, vol. 6, pp. 311–335, 1998.

Sema Dumanli (M'11) was born in Elazig, Turkey, in 1984. She received the Bachelors degree in electrical and electronic engineering from Middle East Technical University (METU), Ankara, Turkey, in 2006 and the Ph.D. degree from University of Bristol, Bristol, U.K., in 2010.

From June 2006 to February 2007, she was a Design Engineer at ASELSAN Inc., Turkey. Since August 2010, she has been a Research Engineer at Toshiba Research Europe, Bristol, U.K. Her current research interests include antenna design, propagation channel modelling, MIMO, mm-wave technology and terahertz communications.

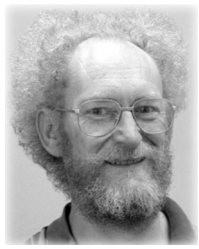

Chris J. Railton received the B.Sc. degree in physics with electronics from the University of London, London, U.K., in 1974 and the Ph.D. degree in electronic engineering from the University of Bath, Bath, U.K., in 1988.

During 1974 to 1984, he worked in the Scientific Civil Service on a number or research and development projects in the areas of communications, signal processing and EMC. Between 1984 and 1987, he worked at the University of Bath, on the mathematical modeling of boxed microstrip circuits. He currently works in the Centre for Communications Research, University of Bristol, where he leads the Computational Electromagnetics Team which is engaged in the development of new algorithms for electromagnetic analysis and their application to a wide variety of situations including planar and conformal antennas, microwave and RF heating systems, radar and microwave imaging, EMC, high speed interconnects and the design of photonic components.

Dominique L. Paul (M'03) received the D.E.A. degree in electronics from Brest University, Brest, France, in June 1986 and the Ph.D. degree from Ecole Nationale Superieure des Telecommunications de Bretagne (LEST-ENSTBr), Brest, France, in January 1990.

From 1990 to 1994, she was a Research Associate at the Centre for Communications Research, University of Bristol, Bristol, U.K. During 1995 to 1996, she worked as a Research Associate at the Escuela Tecnica Superior de Ingenieros de Telecomunicacion of Madrid, Spain, under a grant from the Spanish Government. Since 1997, she has been a Research Fellow in the Centre for Communications Research, University of Bristol, Bristol, U.K., with a permanent position from 2003. Her research interests include the electromagnetic modelling of passive devices such as microwave heating systems, dielectric structures at millimeter wavelengths, MIMO systems, low profile antennas, conformal antenna arrays and textile antennas for wearable applications.

Dr. Paul is a member of the IET, IEEE Microwave Theory and Techniques Society and IEEE Antennas and Propagation Society.